# Dust and Infrared Polarization Signatures

D. K. Aitken

*Division of Physical Sciences, University of Hertfordshire, College Lane,
Hatfield, HERTS AL10 9AB, UK*

**Abstract.**     An outline is presented of observations and interpretations of polarization in the near and mid-infrared. Grain alignment occurs in the diffuse interstellar medium, in dense and massive molecular clouds and in HII regions as well as the boundaries of diffuse quiescent clouds; the resulting polarization displays features due to thermal excitation of molecular bonds and these are discussed in terms of grain chemistry and physics and the grain environment.

In the near-infrared scattering can be a complicating factor, and at longer wavelengths polarization may be a combination of absorption and emission. Spectropolarimetry can separate these contributions and provide information on fractionation of grain material and ambient conditions along the line-of-sight. It also provides evidence on grain chemistry independent of, and more sensitive than, spectroscopy. Polarimetry also reveals magnetic field directions projected on the sky.

The gains from large 10m class telescopes are particularly large in this wavelength region but not yet exploited, in spite of the availability of relevant instrumentation. Some of these will be outlined.

## 1.    Introduction

Molecular vibrations in dust grains give rise to absorption features mainly in the range 2.5–25 $\mu$m, often referred to as the 'thermal infrared'. The features are characteristic of the chemical bonds involved and offer a means of determining the chemistry of dust grains through infrared spectroscopy of astronomical sources. However the spectra are complicated by the frequent presence of emission as well and of other contributions such as the often poorly defined underlying spectrum, and by the physical structure of the grains themselves. An alternative and complementary method is to use spectropolarimetry, which effectively selects only the contributions from the dust grains.

The polarization is attributed to a degree of alignment of aspheric grains which causes a difference in extinction between two orthogonal directions along the line-of-sight, known as 'dichroism' of the medium. Determination of polarization entails the measurement of intensity in several planes of polarization, and rather than rotate a polarization analyser it has become established practise in the thermal infrared use a waveplate to rotate the incoming plane of polarization together with a fixed analyser before the detection array. This method eliminates instrumental polarization occurring after the waveplate. Ideally, orthogonal planes of polarization are measured simultanteously using, for instance, a Wollaston prism, thus avoiding spurious polarizations introduced by changes of sky noise and seeing, as well as more efficient use of time. Such a method

is described by Packham & Hough (these proceedings) and will be used by CanariCam, a mid-IR instrument on the the 10m telescope, GranTeCan. Because currently available prism materials allow only small beam separations, rapid sequential observations of orthogonal polarizations will probably still be necessary for imaging fields of much more than a few ascseconds.

Grains tend to spin about their short axes, develop a dipole moment in this direction (Barnett effect) and precess about the ambient field. This does not constitute alignment since in an isotropic distribution all spin angles are equally likely, but any lack of isotropy results in the average spin direction being either parallel to or orthogonal to the field. Where it can be checked it has always been parallel to the field.

E-vectors parallel to grain long axes will be attenuated more strongly and polarization from cold grains will then be along the the projection of the magnetic field on the plane of the sky; warm emitting grains will produce polarization orthogonal to this. Fortunately emission and absorption have different polarization profiles and spectropolarimetry or observations at more than one wavelength can, in many cases, separate these contributions (Aitken et al. 2004).

For polarization the difficulty is the smallness of the signals. Polarizations are typically only a few percent and to measure this to 10%, or equivalently a few degrees in position angle, requires observations to a signal/noise $\simeq 500$ at each of the three or four waveplate positions. Largely because of this the accessible sources studied in this way are only of order one hundred in the thermal infrared and consequently statistics are not good; this situation will be improved only with access to large telescopes.

## 2.  The Polarization Spectra

The difference in extinction,

$$\Delta\tau(\lambda) = \tau_x(\lambda) - \tau_y(\lambda),$$

where $\tau_x$ is taken as parallel to a long grain dimension, produces by absorption the polarized intensity:

$$P_a(\lambda) = I_0(\lambda)(e^{-\tau_x(\lambda)} - e^{-\tau_y(\lambda)})$$

where $I_0(\lambda)$ is the source spectrum. The polarized fraction is:

$$p_a(\lambda) = \frac{e^{-\tau_x(\lambda)} - e^{-\tau_y(\lambda)}}{e^{-\tau_x(\lambda)} + e^{-\tau_y(\lambda)}} = -\tanh(\Delta\tau(\lambda)/2)$$

so

$$p_a(\lambda) \simeq -\Delta\tau(\lambda)/2 \tag{1}$$

to the approximation that $\Delta\tau(\lambda)/2 = (\tau_x(\lambda) - \tau_y(\lambda))/2$ is small, and since $p_a(\lambda)$ is rarely more than 10% could well be considered an equality. The negative sign indicates that the polarization is in the direction of least extinction, in this case the $y$ direction. $\tau_x(\lambda)$ and $\tau_y(\lambda)$ are different functions of the dielectric function, $\epsilon(\lambda)$, depending on geometry, and not merely scalings of each other, and while the resultant polarization features are similar to the corresponding absorption features they have significant differences and so offer additional and independent

information on grain chemistry. In particular the polarization feature occurs at a slightly longer wavelength, discriminating dichroism from the possibility that the feature is due to scattering, and is more sensitive to fine structure in the dielectric function. For obvious reasons the source spectrum cancels out, so long as it is unpolarized.

For optically thin emission the polarized intensity is:

$$P_e(\lambda) = B(\lambda, T)(\tau_x(\lambda) - \tau_y(\lambda))d\Omega$$

where $B(\lambda, T)$ is the Planck function. Neglecting temperature changes along the line-of-sight the Planck function cancels and the polarized fraction is then:

$$p_e(\lambda) = \frac{\tau_x(\lambda) - \tau_y(\lambda)}{\tau_x(\lambda) + \tau_y(\lambda)} = \frac{\Delta\tau(\lambda)/2}{\tau(\lambda)}$$

$$p_e(\lambda) \simeq -\frac{p_a(\lambda)}{\tau(\lambda)}. \tag{2}$$

$p_a(\lambda)$ and $p_e(\lambda)$ are different functions of $\lambda$ which depend only on the properties of the grains and their alignment.

The polarization position angle, $\theta_a = 0.5\tan^{-1}(u_a(\lambda)/q_a(\lambda))$, are independent of $\lambda$ since the Stokes parameters $q_a(\lambda)$ and $u_a(\lambda)$ differ by only a scale factor, and similarly for $\theta_e$. This is still true even if there is a twist in the alignment direction along the line-of-sight as long as there is no fractionation of grain properties. In this case $\theta$ is some average of the alignment directions along the line-of-sight.

If emission and absorption occur along the same line of sight $q(\lambda)$ is a linear combination of $q_a(\lambda)$ and $q_e(\lambda)$ (we are neglecting products of small quantities) and $u(\lambda)$ is in general a different linear combination of $u_a(\lambda)$ and $u_e(\lambda)$ so that the form of $p(\lambda)$ differs from $p_a(\lambda)$ and $p_e(\lambda)$ and the position angle is no longer independent of $\lambda$. Comparison of Equations 1 and 2 shows that the profiles are significantly different and the two contributions can often be separated (Aitken et al. 2004) in the MIR.

## 3.   Observations

At the time of writing the most comprehensive collection of MIR spectropolarimetry is that of Smith et al. (2000; SWARH) and at shorter wavelengths a series of papers by Hough and associates (Hough et al. 1989, 1996, Chrysostomou et al. 1996). These have concentrated on the most ubiquitous infrared polarization features: the 9.7 $\mu$m silicate absorption feature, which peaks in polarimetry at near 10.3 $\mu$m, and the $H_2O$ ice feature, where again there is a small shift between the polarization peak and the extinction minimum, confirming dichroism (Martin, 1975). In dense clouds these polarization features are often observed along the same line-of-sight but in the diffuse ISM the $H_2O$ ice feature is absent. Clearly silicate grains can be aligned and can act as cores for $H_2O$ ice as mantles.

### 3.1.   Silicates

SWARH presented spectropolarimetry from 8–13 $\mu$m of 38 Galactic sources, 3 Galactic Centre Quintet sources, 13 regions in SgrA and a Seyfert galaxy NGC1068; Six of these were also observed from 16–21 $\mu$m. A dozen or so of the Galactic sources show absorptive polarization uncontaminated by emission and the form of $p_a(\lambda)$ for silicate dust in the 10 $\mu$m region (O–H stretch) is usually taken from one of them, the BN object in OMC-1, since this is well defined, has high signal/noise, and fits acceptably well other sources with high extinction. Purely emissive polarization is poorly represented in the study of SWARH, RCW38 being the only assignment and of low signal/noise, and its profile is better found using equation 2 and taking $\tau(\lambda)$ from observations of the Trapezium in Orion (Gillet et al. 1975). Alternatively there are several sources in SWARH containing both emission and absorption of sufficient S/N to allow separation into either $q$ or $u$ merely by coordinate rotation, and these profiles give added weight to the $p_e(\lambda)$ derived from $p_a(\lambda)$ and $\tau(\lambda)$. The $p_a(\lambda)$ and $p_e(\lambda)$ profiles are shown in Figure 1.
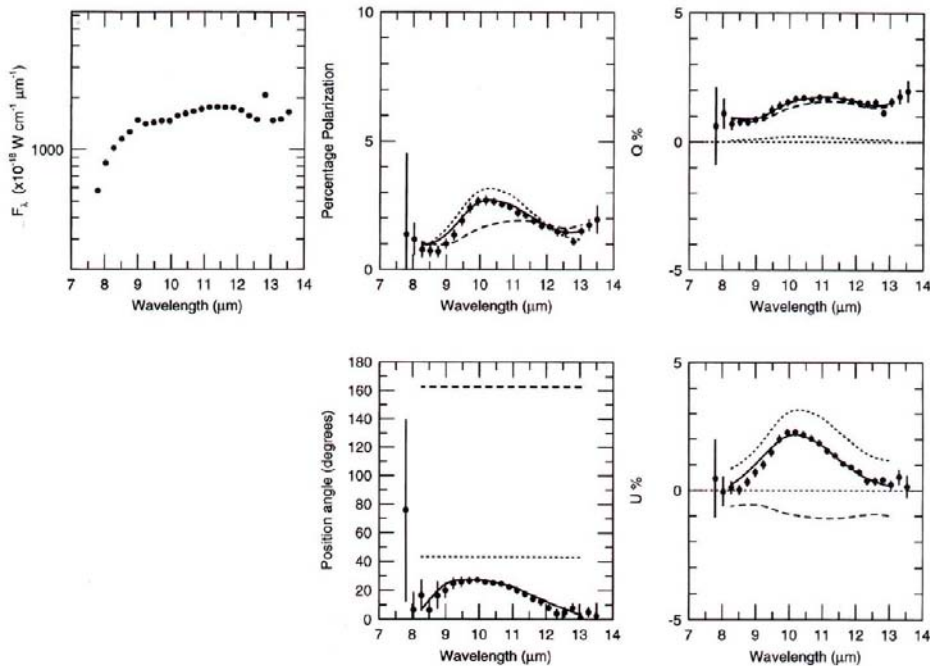


Figure 1.    Fit to G333.6-0.2 by a linear combination of the Stokes parameters of $p_a$ (dotted) and $p_e$ (dashed). Emission lines of A[III] and [NeII] are at 9.0 and 12.8 $\mu$m. (Smith et al. 2000)

About 70% of the Galactic sources satisfy the two component model of cold and warm silicate grains using these profiles (Aitken et al. 2004). Figure 1 shows such a fit for the HII region G333.6-0.2 where there is a twist of 30° between the HII region and the cold overlying dust. All of the Galactic Centre sources are fit by this model, though with slightly narrower $p_a(\lambda)$ than BN. Spectroscopy has shown that silicates are amorphous in dust grains and this is supported by the

smooth polarization profiles too, with one exception, the bipolar YSO GL2591. Here there is a narrow polarization peak at 11.2 $\mu$m, attributed to olivine, with no observed structure in the intensity spectrum. Recently Wright et al. (2002) has shown that the crystallinity exists as inclusions within more usual silicate material.

Two of the Galactic sources are Wolf-Rayet stars and probably represent the diffuse interstellar medium (DISM). Their polarization FWHM profiles $\simeq 2.5\,\mu$m are slightly narrower than the 3.0 $\mu$m for BN and similar to the Galactic Centre sources.

There are three Carbon stars within the sample: two of them have flux spectra showing SiC in absorption and these have a small but significant polarization which peaks weakly between 11 and 13 $\mu$m and if attributed to aligned SiC grains implies a specific polarization $p/\tau \sim 5\%$ compared with the typical value of $\simeq 2\%$ for silicates where the maximum $p/\tau$ observed is 4%.

A summary of the SWARH results is shown in Table 1.

Table 1.  Some statistics of Galactic sources from Smith et al. 2000

|         | a+e | a  | e | (a/e/ae) | nofit | total |
|---------|-----|----|---|----------|-------|-------|
| YSO     | 5   | 10 | - | 4        | 3     | 22    |
| ISM (WR)| -   | 2  | - | 1        | -     | 3     |
| HII     | 3   | 1  | 1 | 2        | 1     | 8     |
| C       | -   | -  | - | -        | 3 SiC | 3     |
| others  | 1   | -  | - | 1        | -     | 2     |
|         |     |    |   |          |       | 38    |

There is a clear preference for the absorptive polarization position angle to be associated with the Galactic plane, as expected from previous optical studies, but the field associated with emissive polarization shows no such preference, admittedly with much poorer statistics. Where both emissive and absorptive polarization is present along the same line-of-sight there is considerable scatter of field angle between the emissive and absorptive regions with an rms scatter of 50°. The emissive regions are presumably more evolved and disturbed than the overlying medium.

Most of these observations are of objects within dense clouds with $1 < \tau_{10\mu m} < 5$ and $A_V \gg 10$mag. The specific polarization $p_a/\tau \simeq 2\%$ is based on alignment along this whole path of extinction; if only a small 'special' fraction of it is involved in alignment, as has been suggested, then its specific polarization would become much larger. The specific polarization $p_e$, obtained directly from emission and independent of optical depth, is also $\simeq 2\%$, with a spread up to 4%. It appears that the alignment is a general property of massive dense clouds rather than peculiar parts of them. The Galactic Centre sources, SgrA and the

GCS quintet sources lie along a path of order $30A_V$, or $\tau_{sil}$ in the range 3–4, and have $p_a/\tau$ in the range 2–3% similarly evaluated, so the same arguments apply to the general interstellar medium. Similar conclusions follow from the work in the FIR and submm by Hildebrand and associates: the large polarizations $\simeq 5\%$ often observed rule out dilution by appreciable fractions of the line of sight.

## 3.2.   Ices

$H_2O$ ice has features at 3.05 $\mu$m (O–H stretch), 6.0 $\mu$m (O–H–O bend) and 12–14 $\mu$m (libration), and the latter peak position is temperature dependent, moving to shorter wavelengths at higher temperatures. All the features have been observed spectroscopically but only the O–H stretch feature has been observed in polarimetry. Like the silicate feature it is seen most strongly in the BN object and here too the characteristic wavelength shift of dichroism is well seen in Figure 2 (Hough et al. 1996) together with a position angle shift in the feature.
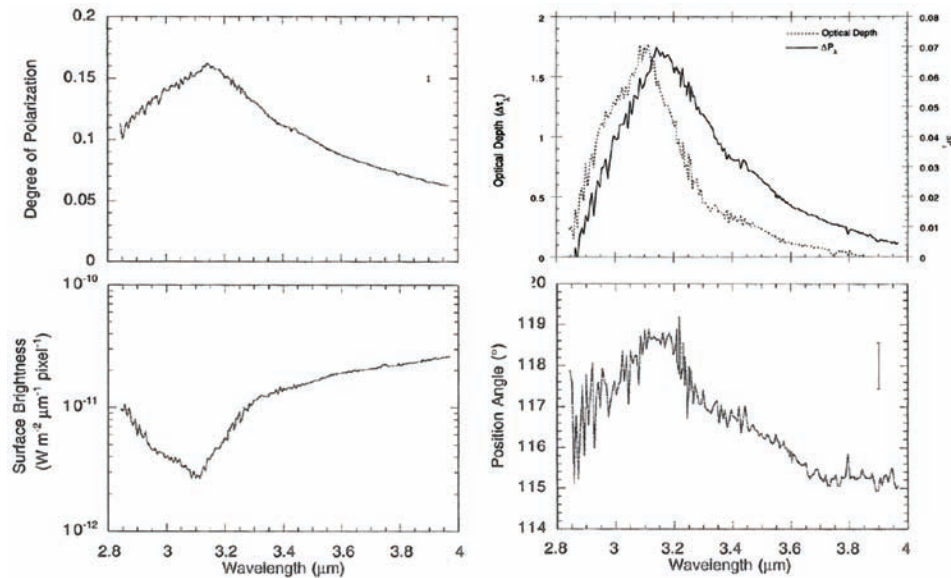


Figure 2.    The 3.1 $\mu$m $H_2$ ice feature in BN. The polarization spectrum is shown top right with intensity below. These are compared after continuum subtraction top right and the position angle spectrum is shown below.

The feature has a long wavelength wing in both spectroscopy (eg Whittet 2003 and references therein) and spectropolarimetry, and is not yet completely explained, though mixtures of other ices play a part.

Currently only nine sources have spectropolarimetry through 2–13 $\mu$m, covering the ice and silicate features. These are presented by Holloway et al. (2002) and the association between the features discussed. All the features are seen in absorption and polarization except in GL2591 which, while it has silicate absorption and polarization and ice absorption, lacks the ice polarization feature.

If ice exists as mantles on silicate cores, as is generally assumed, we expect good correlations between position angles and polarization in the features. The

correlation is good (R=.97) when position angles of the ice and silicate features are compared, slightly less so for the ice and silicate polarizations (R=.77) but poor for their specific polarizations (R=.17). The slightly poorer correlation for polarization suggests a relatively small variation in the mantle/core ratio in the sample. There is some uncertainty in the estimates of $\tau_{sil}$ due to the uncertain underlying spectrum, and also in $\tau_{ice}$ due to the correction for telluric effects around and short of 3 $\mu$m, and these factors probably account for the poor correlation of specific polarizations.

Many of the ice polarization features show a position angle shift with respect to the 3 $\mu$m continuum. Typically BN has a feature polarization of 16% at a position angle of 119° and continuum polarization of 9% at 115° (interpolated) giving an observed shift of 4°; the feature is of course a combination of ice and silicate and subtraction of the latter's Stokes components gives the ice contribution as 7.2% at 124°. A simple way this could arise is through two separate contributions along the line of sight, a region of bare silicate, at $\theta_A$, and another of core + mantle, at $\theta_B = 124°$. Each of these in turn are averages along their lines of sight. Only $\theta_B$ and the resultant continuum polarization and position angle are known so there is no unique solution, but a range of possibilites:

silicate along B of $\quad p_B$=7% $\quad$ then $p_A$=3.2% at 94° $\qquad$ (as ice)
$\qquad\qquad$ " $\qquad\quad$ $p_B$=4% $\quad$ then $p_A$=5.3% at 108°
$\qquad\qquad$ " $\qquad\quad$ $p_B$=10% $\quad$ then $p_A$=3.1% at 65°
$\qquad\qquad$ " $\qquad\quad$ $p_B$=0% $\quad$ then $p_A$=9.0% at 115° $\quad$ (no mantle)
$\qquad\qquad$ " $\qquad\quad$ $p_B$=20% $\quad$ then $p_A$=11.5% at 40° $\qquad$ .

(This is best viewed graphically in vector form in Stokes qu space.) Plausibly the silicate core has a change of direction 30±15°, and more than this for a more realistic model. Such twists along the line-of-sight are in fact required because of the observed circular polarization seen at short wavelengths (Lonsdale et al. 1980).

Solid CO has a C-O stretch vibration mode at 4.67 $\mu$m and there is a stronger and broader feature at 4.62 $\mu$m attributed to the C-N bond in an unidentified material dubbed XCN. Such structures can only exist within very cold and dense dark clouds where there are no optical/UV photons and grain and gas tmperatures are tightly coupled. Their observed polarization in W33A (Chrysostomou et al. 1996) is a severe test of grain alignment mechanisms. A small dichroic shift of wavelength is observed and the specific polarizations for CO and XCN are $\simeq$ 1% and $\simeq$2.3% respectively, comparable to 1.75% for silicate in the same source and at similar position angle.

## 3.3.   Refractory Features

While ices are generally absent from the diffuse ISM there are a number of refractory hydrocarbon absorption features. One of these is the 3.4 $\mu$m C-H stretch feature which is seen in absorption towards the Galactic Centre. Its polarization has been looked for in the Galactic Centre source IRS7 (Adamson et al. 1999) but no feature polarization excess found at a factor 5 below that expected by comparing the strength of the absorption feature and the assumption that the material is in the form of a mantle on the aligned silicate grains in this path in the ISM. A similar result is found for IRAS 18511+0146 by Ishii et al. (2002). These result argue that here and, by extension, other paths the hydrocarbons

exist as separate entities and not in the form of mantles on silicates (Adamson et al. 1999). Another suggestion is that mantle shapes other than confocal with the core, as usually assumed (for computational convenience), may lead to a much wider range of expected feature polarization. Li and Greenberg (2002) have tested this numerically by comparing confocal and equal eccentricity mantles over a wide range of $a/b$ ratios and mantle/core ratios but the likely spread of the predicted polarization was quite narrow, from 0.7 to 1.2 of the silicate specific polarization. More data here are needed but bright sources suffering large extinction by the ISM are scarce.

## 4.   Modelling the Features

Spectropolarimetry is a more reliable guide to the nature of dust grains than spectroscopy since many of the irrelevant hard to quantify contributions are divided out, and often the polarization profile is more sensitive to minor constituents and can separate line-of-sight effects. The polarization profile can also be interpreted in terms of the band strength of the resonance (eg Hong and Greenberg 1980).

Modelling the polarization profile of the features depends on grain chemistry, its inclusions and mantles, grain shape, mantle shape and thickness, porosity, physical condition such as crystalinity; many parameters are involved. Analytic expressions offer physical insight into the effects of geometry and chemistry but exist only for spheroidal grains in the dipole approximation. For a grain of volume V and complex dielectric function $\epsilon(\lambda) = \epsilon_1(\lambda) + j\epsilon_2(\lambda)$ the cross section is (van de Hulst 1957):

$$C_{a,b} = \frac{2\pi V}{\lambda} \frac{\epsilon_2(\lambda)}{[L_{a,b}(\epsilon_1(\lambda) - 1) + 1]^2 + [L_{a,b}\epsilon_2(\lambda)]^2} \qquad (3)$$

where $C_{a,b}$ is the cross section for **E** vectors parallel to the symmetry axis, $a$, or orthogonal to it, $b$. $L_{a,b}$ is a geometrical factor depending on the ratio $a/b$ and $L_a + 2L_b = 1$ for spheroidal grains and $a < b$ for oblate grains. This expression has been extended to include confocal mantles (Gilra 1972). These expressions, together with the "astronomical silicate" dielectric function constructed by Draine and Lee (1984) from the then available astronomical and laboratory data, has been successful in reproducing the salient features of the polarization profiles and serves as a starting point for further work. Grains are almost certainly irregular and numerical techniques such as the "discrete dipole approximation" (DDA) (Purcell and Pennypacker 1973) exist to approximate grains of arbitrary shape and inhomogenous structure and chemistry, and mixtures and inclusions can be dealt with by "effective medium theory" (EMT) (eg Bohren and Huffman 1983).

Hildebrand and Dragovan (1995) used the "astrosilicate" dielectric function and equation 3 to infer that oblate grains give a better fit to the observed profile than prolate and require only mild oblateness with an $a/b \simeq 1/2 - 2/3$. A gaussian distribution of mildly oblate and prolate grain shapes without bias towards either kind of spheroid produces similar profiles (Aitken 1996).

In complete spinning alignment such grains would give 35% polarization at 100 $\mu$m whereas the observed polarization is 1/4 of this corresponding to the

predictions of a Rayleigh reduction factor of 25% as expected from alignment through ambipolar diffusion (Roberge 1996).

Nevertheless none of these profiles based on "astrosilicate" give an adequate fit to the observed profiles and there are significant differences in the wings of the 10 $\mu$m window which become very noticeable when when the treatment is extended to the 20 $\mu$m window.

Recently there have been a number of attempts to tackle the observed discrepancies through modifications of the dielectric function, and the application of numerical techniques to include porosity, mixtures and non-spheroidal shapes. From laboratory studies of terrestrial silicates it is clear that the data favour amorphous material. For the 10 $\mu$m region the (arguably) best fit is from Wright et al. (2002) who show the profile produced by a mixture of 65% amorphous olivine, 10% carbon, 10% porosity and an ice mantle with 25% of the core volume. This is a considerable improvement on astronomical silicate and amorphous olivine alone and this composite fits the BN profile well for the 8–13 $\mu$m region.

The small narrow peak in polarimetry at 11.2 $\mu$m in GL2591 is so far unique to this source. It is not present in its spectroscopy, and was attributed to a more crystaline component (Aitken et al. 1988), possibly olivine although an exact wavelength match with laboratory irradiated olivine was not obtained. There is a similarity to a spectrscopic emission peak in Comet Halley, also attributed to olivine (Bregman et al. 1987). A good wavelength match to olivine has been obtained by Wright et al. (2002) by using EMT to investigate inclusions of crystalline olivine within an "astrosilicate" base, and a good fit to the rest of its 8–13 $\mu$m polarization profile. The 20 $\mu$m region is, however, fit slightly better by astrosilicate alone in GL2591.

A particular problem for astrosilicate has been the 20 $\mu$m profile of the BN object (Aitken et al. 1989) which exceeds the predicted polarization by a factor of 1.5. Laboratory analogues such as glassy bronzite (Dorschner et al. 1988) improved the (19/10) $\mu$m peak ratio but at the expense of increasing the peak wavelength by 2 $\mu$m. Henning & Stognienko (1993) investigated the effects of using composite grains (Mathis & Wiffen 1989) with porosity. Using DDA analysis they found that while the 19/10 ratio is increased there is also a peak wavelength shift and that compact grains are better than porous, and that composite grains of graphite and silicate produce profiles that are too broad. Mantles of ice, carbon (O'Donnell 1994), tholins (Khare & Sagan 1994) all produce shifted peak wavepengths and too broad features. Greenberg & Li (1996) have used an amorphous olivine core with a refractory mantle of UV irradiated organic hydrocarbon material. This produces a plausible match to the height of the observed feature but with a peak at 18 $\mu$m rather than the observed 19 $\mu$m, and the match is poor shortwards of 9 $\mu$m. Iron-magnesium oxides also increase the 19/10 polarization ratio and Wright et al. (2002) have used dielectric function data of Henning et al. (1995) and Roessler & Huffman (1991) for pure magnesium oxide inclusions and produce different approximations to the observed profile.

It is curious that astronomical silicate itself produces as good a match to the observed 19 $\mu$m peak position as the other models and it is well to consider what other factors than chemistry may lead to the observed 19/10 ratio. Changes in this ratio do occur with changing view angle and field configuration in some

of the disk models of Aitken etal (2000), based on astrosilicate, but these do not give such an enhancement of the 19/10 ratio as observed. It is also well to remember the very limited statistics available: spectropolarimetry at 10 and 20 $\mu$m is available for only six molecular cloud sources and of these only two appear to be uncomplicated by emission and one of these has a so-far unique 8–13 $\mu$m profile!

Modelling of the $H_2O$ ice feature in BN (Hough et al. 1996) shows that a mix of ices with $H_2O$:$CH_3OH$:$CO$:$NH_3$ in the ratio 100:50:1:1 (the STRONG mixture of Hudgins et al. 1993) as a mantle on silicate core is necessary to fit the long wavelength wing of the feature with a possible additional carbonaceous bump at 3.47 $\mu$m. The solid CO feature at 4.67 $\mu$m also appears to be a composite of CO and $H_2O$ ices (Chrysostomou et al. 1996)

## 5.  Polarimetric Imaging

Polarimetry is often the only way to study the magnetic fields in dense objects. In the thermal infrared it allows high spatial resolution of warm inner regions but care has to be taken to identify and separate emission from absorption. Spot checks with spectropolarimetry may reveal a nearly uniform dichroic screen through which an inner region is viewed. Such is the case for the SgrA filaments where the overlying absorptive component is well known (Aitken et al. 1996, SWARH) and can be used to correct polarimetric imaging at 12.5 $\mu$m, where emissive polarization dominates (Aitken et al. 1998, Glasse et al. 2003). The field structures are aligned along the ionized filaments and seem to result from the tidal shearing of the ionised material as it falls around SgrA$^\star$. Similar techniques have been applied to the HII region G333.6-0.2 (Fujiyoshi et al. 2001). More generally, more than one wavelength would be needed to identify and separate the polarization components (Aitken et al. 2004).

## 6.  Conclusions and Future Prospects

Near and mid-infrared polarimetry is a sensitive and powerful probe of the nature of grains and their mantles, yielding detailed information on their shape, chemistry and physical structure, and direction of the ambient magnetic field projected on the sky.

Amorphous olivines with icy mantles of $H_2O$ and $CH_3OH$ provide the best fits to grains in molecular clouds while in the diffuse ISM the ices are replaced by hydrocarbons which do not appear to be mantles on the silicates but rather form a separate population. Crystallinity is rare in the ISM and molecular clouds, being observed as a constituent in only one out of forty odd lines of sight. There is evidence that SiC grains can be aligned.

Alignment seems ubiquitous: as well as the outer regions of diffuse clouds, it occurs throughout dense and massive molecular clouds, the general interstellar medium, and HII regions. It gives the direction of magnetic fields and sometimes fractionation of material along the line of sight, and the inner structure of star forming regions.

Polarimetry statistics are sparse in this wavelength region; sampling of some objects is in the one's and two's and many other classes have not been observed

because of lack of flux; so it has remained in spite of 10m class telescopes, appropriate instrumentation and very large gains in signal/noise ratio. Real progress can only be made through access to these more and longer lines of sight to build up a proper census of the Galaxy and to extend to other galaxies, especially those with obscured active nuclei.

## References

Adamson, A.J., Whittet, D.C.D., Chrysostomou, A., Hough, J.H., Aitken, D.K., Wright, G.S., & Roche, P.F. 1999, ApJ, 512, 224

Aitken D.K. 1996, in ASP Conf. Ser., Vol 97, Polarimetry of the Interstellar Medium, Ed. W.G.Roberge & D.C.B.Whittet, (San Francisco: ASP), 225

Aitken, D.K., Smith, C.H., & Roche, P.F. 1989, MNRAS, 236, 919

Aitken, D.K., Hough, J.H., Roche, P.F., Smith, C.H., & Wright, C.M. 2004, MNRAS, 348, 279

Aitken, D.K., Roche, P.F., Smith, C.H., James, S.D., & Hough, J.H. 1988, MNRAS, 230, 629

Aitken, D.K., Efstathiou, A., McCall, A., & Hough, J.H. 2002, MNRAS, 329, 647

Aitken, D.K., Smith, C.H., Moore, T.J.T., & Roche, P.F. 1996, in ASP Conf. Ser. V102. The Galactic Center, ed R.Gredel, 179

Aitken, D.K., Smith, C.H., Moore, T.J.T., & Roche, P.F. 1998, MNRAS, 299, 743

Bregman, J.D., Campins, H., Witteborn, F.C., Wooden, D.H., Rank, D., Allamandola, L.J., Cohen, M., & Tielens, A.G.G.M. 1987, A&A, 187, 616

Bohren, C.F., and Huffman, D.R. 1983, Absorption and Scattering of Light by Small Particles, (New York,: Wiley)

Chrysostomou, A., Hough, J.H., Whittet, D.C.B., Aitken, D.K., Roche, P.F., & Lazarian, A. 1996, ApJ, 465, L61

Dolginov, A.Z., & Mytrophanov, L.G. 1976, Ap&SS, 43 291

Dorschner, J., Freidmann, C., Gurtler, J., & Henning, Th. 1988, A&A, 198, 223

Draine, B.T., & Lee, H.M. 1984, ApJ, 285, 89

Fujiyoshi, T., Smith, C.H., Wright, C.M., Moore, T.J.T., Aitken, D.K., & Roche, P.F. 2001, MNRAS, 327, 233

Gillet, F.C., Forrest, W.J., Capps, R.W., & Soifer, B.T. 1975, ApJ, 200, 609

Gilra, D.P. 1972, in The Scientific Results from OAO-2, ed A.D.code (NASA, SP310), 295

Glasse, A.C.H., Aitken, D.K., & Roche, P.F. 2003, in The Central 300pc of the Milky Way, Ed. A.Cotera, S.Markoff, T.R.Geballe, & H. Falke. Astron. Nachr., 324, 563

Greenberg, J.M.& , Li, A. 1996, A&A, 309, 258

Henning, Th., & Stognienko, R. 1993, A&A, 280, 609

Henning, Th., Begemann, B., Mutschke, H., & Dorschner, J. 1995, A&A Sup. Ser., 112, 143

Hildebrand, R.H., & Dragovan, M. 1995, ApJ, 450, 663

Holloway, R.P., Chrysostomou, A., Aitken, D.K., Hough, J.H., & McCall, A. 2002, MNRAS, 336, 425

Hough, J.H., Whittet, D.C.B., Sato, S., Yamashita, T., Tamura, M., Nagata, T., Aitken, D.K., & Roche, P.F. 1989, MNRAS, 241, 71

Hough, J.H., Chrysostomou, A., Efstathiou, A.N., Messinger, D., Whittet, D.C.B., Aitken, D.K., & Roche, P.F. 1996, ApJ, 461, 902

Hong, S.S., & Greenberg, J., M. 1978, A&A, 69, 341

Hudgins, D.M., Sandford, S.A., Allamandola, L.J., & Tielens, A.G.G.M. 1993, ApJS, 86, 713

Ishii, M., Nagata, T., Chrysostomou, A., & Hough, J.H. 2002, AJ, 124, 2790

Khare, B.N., & Sagan, C. 1984, Icarus, 60, 127

Li, A., & Greenberg, J., M. 2002, ApJ, 577, 789

Lonsdale, C.J., Dyck, H.M., Capps, R.W., & Wolstencroft, R.D. 1980, ApJ, 238, L31

Martin, P.G. 1975, ApJ, 202, 393

Mathis, J.S., & Whiffen, G. 1989, ApJ, 341, 808

O'Donnell, J.E. 1994, ApJ, 437, 262

Purcell, E.M., & Pennypacker, C. R. 1973, ApJ, 186, 705

Roberge, W.G. 1996, in ASP Conf. Ser. Vol 97, Polarimetry of the Interstellar Medium, Ed. W.G.Roberge & D.C.B.Whittet, (San Francisco: ASP), 401

Roessler, & Huffmann. 1991, *Magnesium Oxide (MgO)*, in Handbook of Optical Constants of Solids II, ed Edward D. Palik, Academic Press, 919

Smith, C.H., Wright, C.M., Aitken, D.K., Roche, P.F., & Hough, J.H. 2000, MNRAS, 312, 327 (SWARH)

Wright, C.M., Aitken, D.K., Smith, C.H., Roche, P.F., & Laureijs, R.J. 2002, In The Origins of Stars and Planets: the VLT View. Ed. J.F.Alves & M.J.McCaughrean, (Springer-Verlag), pp85